

Nonlinear Dynamical Behaviors of the Equilibrium Longitudinal Distribution by Localized Wakes in an Electron Storage Ring

S.-H. Park^{*,1,†} H.-Ch. Kim^{1,‡} J.K. Ahn^{1,§} and E.-S. Kim^{2,¶}

¹*Department of Physics & Nuclear Physics and Radiation Technology Institute (NuRI),
Pusan National University, Busan 609-735, Korea*

²*Pohang Accelerator Laboratory, POSTECH,
San 31, Pohang, Kyungbuk 790-784, Korea*

Abstract

We investigate the effects of a localized constant wake and a localized linear wake on the longitudinal beam distribution in equilibrium. We also examine the effects of the composite wake on the particle distribution when the constant wake and linear wake simultaneously exist in the ring. While moving around the parameter space, the system can show bifurcation phenomena and transition features between periodic states. We study the dynamical states in a beam, using the multi-particle tracking method in a Gaussian approximation. They show good qualitative agreement.

PACS numbers: 29.20.Dh

Keywords: wakes, bifurcation, electron storage ring, multi-particle tracking

* Present address: LG.PHILIPS LCD, 161, Imsoo-dong, Kumi, Kyungbuk 730-350, KOREA

†Electronic address: shpark@lgphilips-lcd.com

‡Electronic address: hchkim@pusan.ac.kr

§Electronic address: ahnjk@pusan.ac.kr

¶Electronic address: eskim1@postech.ac.kr

I. INTRODUCTION

When a beam is stored in a storage ring, the beam is affected by a wake force that is generated by an electromagnetic interaction between the beam and the components of the ring. The wake force disturbs the distribution of particles in the beam. Various approaches to investigate the particle distribution have been performed. It was usually assumed that the wake force was averaged over one turn and was distributed uniformly in the ring. In fact, however, the wake sources may be localized. Therefore, such assumptions of an averaged and uniform wake force may cause different dynamical behaviors of the system from real ones in many cases. To see the effects due to such position-dependent wake forces, Hirata [1] investigated the particle distribution in a beam, assuming a constant localized wake. Hirata *et al.* [2] then showed that the equilibrium bunch length in electron storage rings could exhibit a cusp-catastrophe behavior. Kim *et al.* [3] found that several multi-periodic states in particle distributions of a beam could also exist for a constant wake.

The aim of the present work is at investigating dynamic behaviors of the longitudinal beam distribution in the presence of the wake that has two components localized at one position of the ring. Here, we consider the linear wake as well as the constant one as sources of the localized wakes. It is also of great interest to see how the longitudinal beam distribution behaves dynamically under the composite constant and linear wakes in a ring. The dynamical behaviors of the beam distribution will be examined with the damping time, the strength of the wake force, and the synchrotron tune considered. It will be shown that the dynamic system under two localized wake sources may present quite different dynamic behavior from that with an individual wake source taken into account.

The paper is organized as follows: In Section 2, we briefly describe the model which is used in order to investigate the equilibrium longitudinal distribution of the beam particles in a Gaussian approximation. In Section 3, we study the dynamical states of the distribution of particles in a beam. To check the validity of the results from the present model, we also compare them with those from the multi-particle tracking in Section 4. Finally, Section 5 is devoted to discussion and conclusion.

II. THE MODEL

A. Longitudinal dynamics

We assume that there are two localized wake sources at one position of the ring. To describe dynamics of the particle distribution in longitudinal phase space, we introduce the following normalized longitudinal variables:

$$x_1 = \frac{\text{longitudinal displacement}}{\sigma_z}, \quad x_2 = \frac{\text{energy deviation}}{\sigma_E},$$

where σ_z is the natural bunch length and σ_E stands for the natural energy spread. The center of the bunch is located at $x_1=0$ such that $x_1 > 0$ corresponds to the rear part of the bunch. The motion of a particle in a ring can then be modeled as follows:

- 1) Radiation

$$\begin{pmatrix} x'_1 = x_1 \\ x'_2 = \Lambda x_2 + (1 - \Lambda^2)^{1/2} \hat{r} \end{pmatrix} \quad (1)$$

2) Wake

$$\begin{pmatrix} x'_1 = x_1 \\ x'_2 = x_2 - \phi(x_1) \end{pmatrix} \quad (2)$$

3) Synchrotron oscillation

$$\begin{pmatrix} x'_1 \\ x'_2 \end{pmatrix} = U \begin{pmatrix} x_1 \\ x_2 \end{pmatrix}, \quad (3)$$

where

$$U = \begin{pmatrix} \cos(2\pi\nu) & \sin(2\pi\nu) \\ -\sin(2\pi\nu) & \cos(2\pi\nu) \end{pmatrix}. \quad (4)$$

In the above equations, $\Lambda = \exp(-2/T_e)$, T_e being the synchrotron damping time divided by the revolution time, ν the synchrotron tune and \hat{r} a Gaussian random variable with zero mean and unit standard deviation.

After one turn in the ring, the motion of a particle is described by

$$\begin{pmatrix} x'_1 \\ x'_2 \end{pmatrix} = U \begin{pmatrix} x_1 \\ \Lambda x_2 + (1 - \Lambda^2)^{1/2} \hat{r} - \phi(x_1) \end{pmatrix}. \quad (5)$$

The wake force is given by

$$\phi(x_1) = \int_0^\infty \rho(x_1 - u) W(u) du, \quad (6)$$

where $\rho(x)$ is the longitudinal charge density normalized to unity, and $W(u)$ stands for the longitudinal wake function multiplied by eQ/σ_E , where e is the electron charge and Q the total charge in a bunch.

In the present work, we consider the constant as well as the linear wake functions: $W(u) = a\Theta(u)$ (Θ being the unit step function) and $W(u) = bu$, where a and b denote the strengths of the wake.

B. Gaussian model

We assume the wake to disappear at a short distance behind the particles producing it so that one can neglect multi-turn effects of the wake. Generally, leading particles in a bunch lose energy due to wake fields. In order to meet this condition, we note that the signs of a and b in the wake functions should be positive.

Since it is not realistic to observe individual particles, we are more interested in statistical quantities such as

$$\bar{x}_i = \langle x_i \rangle, \quad \sigma_{ij} = \langle (x_i - \bar{x}_i)(x_j - \bar{x}_j) \rangle, \quad (7)$$

where i, j are either 1 or 2, which are the moments of the phase-space distribution $\Psi(x_1, x_2)$. In reality, we require all of higher order moments to reproduce $\Psi(x_1, x_2)$. We always approximate $\Psi(x_1, x_2)$ as

$$\Psi(x_1, x_2) = \frac{1}{2\pi\sqrt{\det\sigma}} \times \exp\left[-\frac{1}{2} \sum_{i,j} \sigma_{i,j}^{-1} (x_i - \bar{x}_i)(x_j - \bar{x}_j)\right]. \quad (8)$$

For simplicity, however, we assume here that the distribution function in phase space always remains Gaussian even under the influence of the wake force. We thus need to consider only the first- and second-order moments.

With the same treatment as in Ref. [1] used, each mapping in Eqs. (1)-(3) can be given as :

1) Radiation

$$\bar{x}'_1 = \bar{x}_1, \bar{x}'_2 = \Lambda\bar{x}_2, \quad (9)$$

$$\sigma'_{11} = \sigma_{11}, \sigma'_{12} = \Lambda\sigma_{12},$$

$$\sigma'_{22} = \Lambda^2\sigma_{22} + (1 - \Lambda^2) \quad (10)$$

2) Wake

$$\bar{x}'_1 = \bar{x}_1, \bar{x}'_2 = \bar{x}_2 - \langle\phi\rangle, \quad (11)$$

$$\sigma'_{11} = \sigma_{11}, \sigma'_{12} = \sigma_{12} - \langle(x_1 - \bar{x}_1)\phi\rangle,$$

$$\sigma'_{22} = \sigma_{22} - 2\langle(x_2 - \bar{x}_2)\phi\rangle + \langle\phi^2\rangle - \langle\phi\rangle^2. \quad (12)$$

Further calculations lead us to obtain for the constant wake [2]

$$\bar{x}'_1 = \bar{x}_1, \bar{x}'_2 = \bar{x}_2 - a/2, \quad (13)$$

$$\sigma'_{11} = \sigma_{11}, \sigma'_{12} = \sigma_{12} - a\frac{\sqrt{\sigma_{11}}}{2\sqrt{\pi}},$$

$$\sigma'_{22} = \sigma_{22} - a\frac{\sqrt{\sigma_{12}}}{\sqrt{\pi\sigma_{11}}} + a^2/12. \quad (14)$$

As for the linear wake, we derived the following relations from eqs. (11) and (12)

$$\bar{x}'_1 = \bar{x}_1, \bar{x}'_2 = \bar{x}_2 - b\sqrt{\frac{\sigma_{11}}{\pi}}, \quad (15)$$

$$\sigma'_{11} = \sigma_{11}, \sigma'_{12} = \sigma_{12} - \frac{b\sigma_{11}}{2},$$

$$\sigma'_{22} = \sigma_{22} - b\sigma_{12} + b^2\sigma_{11}(0.608998 + \frac{1}{\pi}). \quad (16)$$

3) Synchrotron oscillation

$$\bar{x}'_i = \sum_j U_{ij}\bar{x}_j, \quad (17)$$

$$\sigma'_{ij} = \sum_{h,k=1}^2 U_{ij}\sigma_{hk}U_{jk}. \quad (18)$$

Note that the mappings for \bar{x}_i and σ_{ij} are related to each other for the constant wake function. However, those for \bar{x}_i depend on σ_{11} for the linear wake function due to the fact that we have utilized the approximation of the Gaussian distribution .

III. DYNAMICAL BEHAVIOR OF THE GAUSSIAN MODEL

If S is the mapping described by Eq. (14) or Eq. (16), then a period-one fixed point $\sigma = (\sigma_{11}, \sigma_{12}, \sigma_{22})$ is defined by

$$\sigma = S(\sigma),$$

while the period-two fixed point is defined by

$$\sigma = S[S(\sigma)]$$

with σ_1 and σ_2 occurring in alternating pairs at successive turns as

$$\sigma_{1,2} = S(\sigma_{2,1}).$$

One can easily extend the definition to period- n states.

First, let us consider the dynamical behavior of the system for the constant wake function. In a previous work [3], one of the authors studied the dynamic states in the parameter space set: $0.01 \leq \nu \leq 0.3$, $1 \leq T_e \leq 1500$ and $0 < a \leq 45$. The results are summarized in Table I, which shows four different behaviors, depending on the synchrotron tune. Those numbers in Table I denote existing period states, i.e. 1 stands for the period-one state, 2 does the period-two state, and 1-2 denotes the period-one and period-two states existing simultaneously. The parameter space shows that several types of equilibrium states such as period-one, period-two, period-three, period-four can exist stably depending on the parameter space (T_e and a).

In the case of the linear wake function, it is shown that the period-one state only exists as an equilibrium state. The tracking of the mapping for the period-one state is drawn in Fig. 1, where the features of the trajectories are indicated near the period-one fixed point. In the left panel of Fig. 1 the fixed point is depicted at $(\sigma_{11}, \sigma_{22}) = (0.53105, 0.53105)$, whereas in the right panel the fixed point is drawn at $(\sigma_{11}, \sigma_{22}) = (0.05341, 0.22875)$.

When it comes to the composite wake of the constant and linear ones ($a\Theta + bu$), Fig. 2 depicts the trackings of the mapping with the different b for $\nu = 0.20$. The system plotted in Fig. 2(a) presents the period-two state, in which the fixed points are located at $(\sigma_{11}, \sigma_{22}) = (15.43191, 17.01573)$ and $(24.96073, 31.95213)$. However, when the strength of the linear wake becomes larger, the number of the fixed points is reduced to one, as shown in Fig. 2(b). Thus the system shows the period-one state that has a fixed point at $(\sigma_{11}, \sigma_{22}) = (6.31035, 9.77105)$.

Figure 3 shows the trackings of the mapping for the composite wake in $\nu = 0.05$. Given $a \neq 0$, $b = 0$, which means that the system is under the constant wake, the system turns out to be in the period-three state. However, when $a \neq 0$ and $b \neq 0$, the system may exist in different states. In the panel (a) of Fig. 3 it is still in the period-three state with $b = 0.01$. In that case, the strength of the linear wake is small so that the system shows similar behavior to the constant wake case. The fixed points are located at $(\sigma_{11}, \sigma_{22}) = (0.78431, 17.25226)$, $(1.257, 2.34851)$ and $(0.35848, 6.9652)$. As the strength of the linear wake becomes larger, the state of the system starts to get changed. When b is 0.5, the system is found in the period-two state with fixed points at $(\sigma_{11}, \sigma_{22}) = (0.26121, 5.89856)$ and $(0.24996, 4.39433)$. If b is set to be 5.0, the system turns back to the period-three state again. The fixed points exist at $(\sigma_{11}, \sigma_{22}) = (6.86404, 17.82114)$, $(2.46592, 32.71493)$ and $(3.61459, 89.64147)$. Putting $b = 7.5$, we find that the system lies in the period-one state. In the panels (a) and (b) of Fig. 4 and in (c),(d) show the equilibrium of σ_{11} for the constant

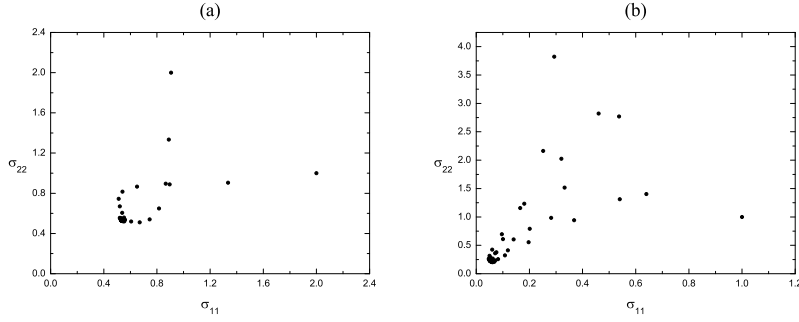


FIG. 1: Features of trajectories for the linear wake. The parameters are initially given for the left panel (a) $T_e = 10$, $b = 0.5$, $\nu = 0.25$, $\sigma_{11} = 2$, $\sigma_{12} = 0$, $\sigma_{22} = 1$, while for the right panel (b) $T_e = 15$, $b = 2.0$, $\nu = 0.05$, $\sigma_{11} = \sigma_{22} = 1$, $\sigma_{12} = 0$.

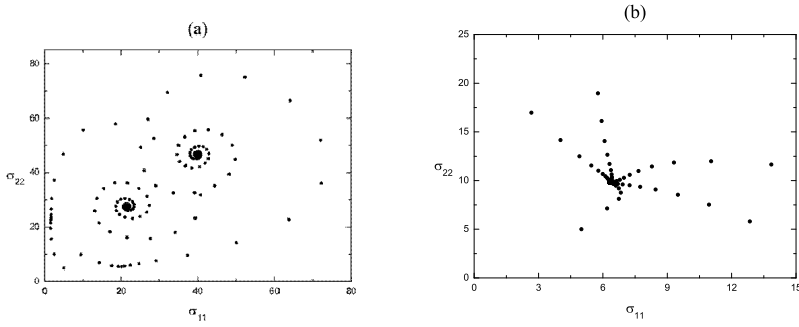


FIG. 2: Features of trajectories for the composite wake. The parameters are initially given as $T_e = 25$, $\nu = 0.20$, $a = 10$, $\sigma_{11} = \sigma_{22} = 5$, $\sigma_{12} = 0$. $b = 0.25$ for the left panel (a), while $b = 1.0$ for the right panel (b).

and the composite wakes with T_e slowly changed, respectively, while in the panels (a) and (c) the equilibrium of σ_{11} is shown when T_e increases from 0 to 30. In the panels (b) and (d) of Fig. 4, we find the processes reversed. There are two transition points in Fig. 4(a): The system shows the transitions from period-one to period-two and then from period-two to period-one. The reverse process for the constant wake is shown in the panel (b) of Fig. 4 and it also has two transition points but the transition states are different from those in the panel (a): It is found that the period-three state changes to the period-two one and vice versa. On the other hand, In the panel (c) of Fig. 4 the composite wake plays a role of changing the period-one to the period-two state and vice versa. In the panel (d) of Fig. 4

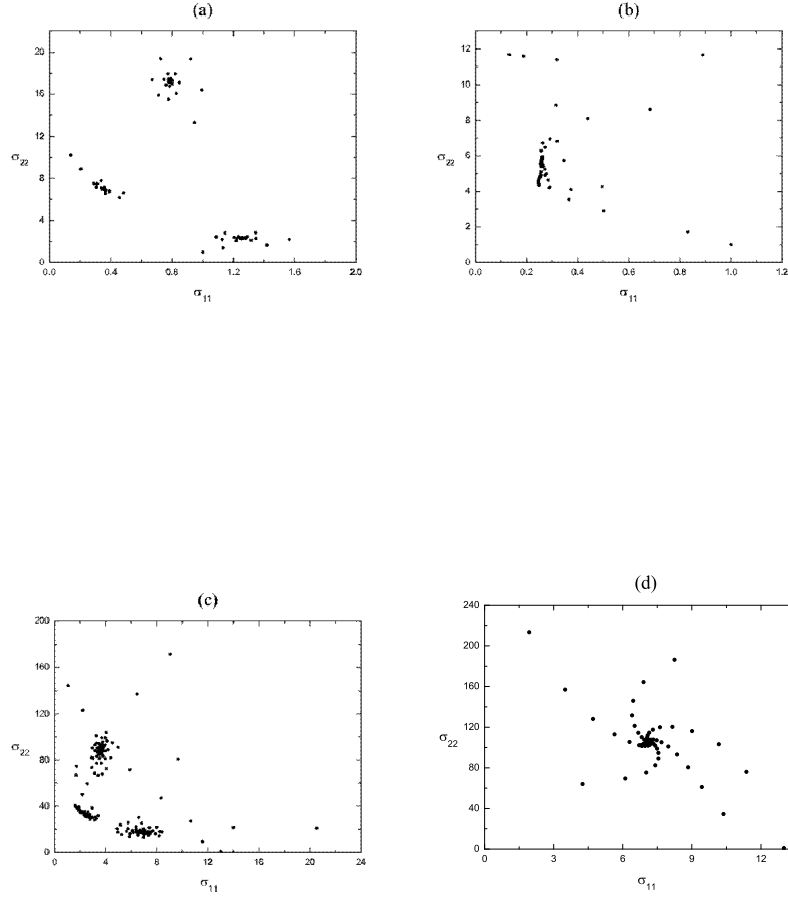


FIG. 3: Features of trajectories for the composite wake. The parameters are initially given as $T_e = 15$, $\nu = 0.05$, $\sigma_{11} = \sigma_{22} = 1$, $\sigma_{12} = 0$, $a = 10$. In the panel (a) $b = 0.01$, while in (b), (c), and (d), $b=0.5, 5.0$, and 7.5 , respectively.

we see the same behavior as in the panel (c).

Trackings of the mapping for the composite wake indicate that when b is small the system turns out to be similar to that for the constant wake, while when the b becomes larger, it changes to another state. Thus, in conclusion, when two different kinds of wakes exist, the dynamical behavior of the system can be changed, depending on the relative magnitude of the strength of the wake: they may show different stability behaviors in the parameter space from the case of a single wake.

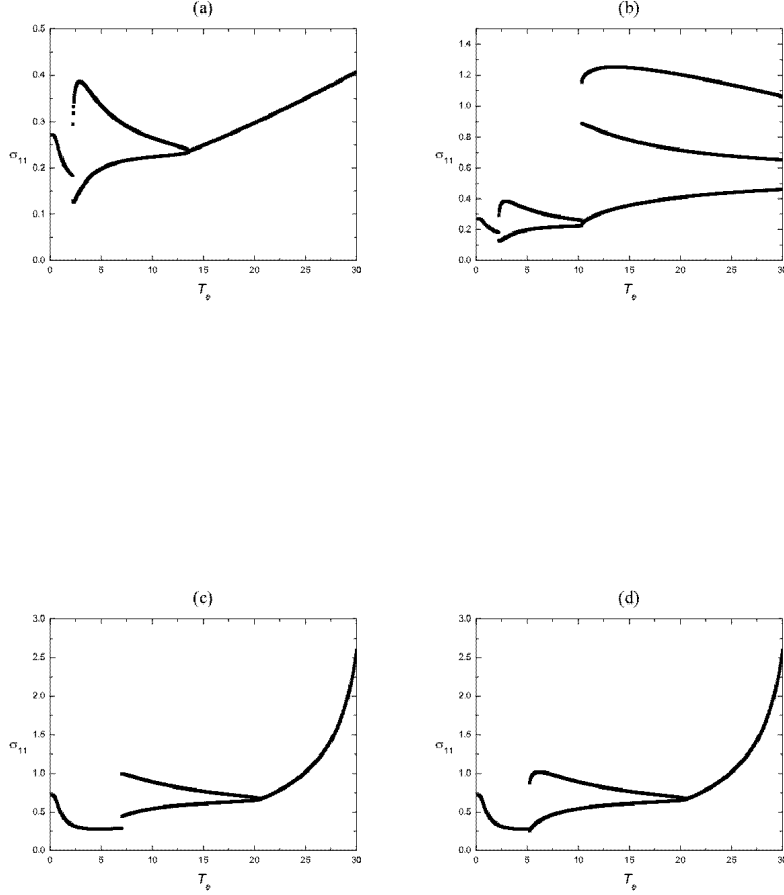


FIG. 4: The bifurcations due to the constant and the composite wakes for $\nu = 0.05$. In the panels (a) and (b) the equilibrium of σ_{11} for the constant wake with the parameters of $a = 10$ and $\sigma_{11} = \sigma_{22} = 1$ and $\sigma_{12} = 0$ are shown, respectively. In the panels (c) and (d) the equilibrium of σ_{11} for the composite wake with the parameters of $a = 10$ and $\sigma_{11} = \sigma_{22} = 1$, $\sigma_{12} = 0$ with $b = 5.0$ are shown. (a) and (c) represent σ_{11} when T_e slowly changes from 0 to 30, and (b) and (d) represent their reverse processes.

IV. MULTI-PARTICLE TRACKING

In this section, we examine the reliability of the results from the present model obtained in Secion 3. The Gaussian Ansatz in the model is considered as a particle distribution of a beam, however, the real distribution can be rather far from the Gaussian one. We thus need to compare the Gaussian distribution with the multi-particle tracking in order to see whether

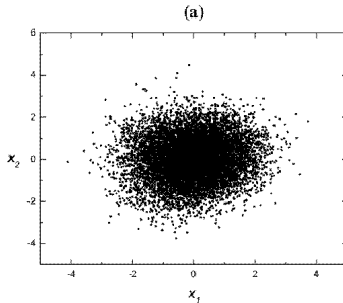


FIG. 5: Phase-space distribution for the period-one state from the multi-particle tracking for the linear wake function. The parameters are given as $T_e = 10$, $\nu = 0.25$, $b = 0.25$ and 20,000 turns. The equilibrium state shows the same distribution per turn.

the results obtained from the model are merely caused by the simplification of the model. In the case of the constant wake function, we use a sorting routine for the calculation of the wake force acting on each particle, i.e. the wake force ϕ that a given particle experiences is obtained by counting the total number of particles preceding it. As for the linear wake function, we calculate individual distances of the preceding particles in order to derive the wake force acting on each particle. Thus, the ϕ is obtained by summing the distances of preceding particles. The initial particle coordinates in the longitudinal phase space are generated as Gaussian random numbers with zero mean and unit standard deviation. We use Eq. (5) to perform the multi-particle tracking in the phase-space coordinates of 10000 macro-particles.

First, we observe the equilibrium states of the particle distribution in the case of the linear wake. The phase space which brings out the multi-particle tracking for $\nu = 0.25$ is depicted in Fig. 5. It is obtained by tracking 10000 particles after 20000 turns. It is shown that the equilibrium state in the multi-particle tracking accounts for the period-one state. It is also examined that the only equilibrium state for the linear wake is found in the period-1 state in the parameter of the synchrotron tunes ranging from 0.01 to 0.3, irrespective of the initial conditions. It is in a good agreement with that of the Gaussian model.

We also find the equilibrium states of the particle distribution due to the composite effect of the constant and the linear wakes. In the panels (a) and (b) of Fig. 6, the phase space yielding the results of the multi-particle tracking for $\nu = 0.2$ is plotted. It is obtained by tracking 10000 particles after 20000 turns. The panels (a) and (b) of Fig. 6 show the period-two state from 19999 turns and 20000 turns, respectively. The equilibrium distributions with the period-two state presents the same distribution by two turns. It is also shown that when b becomes larger, the equilibrium states in the multi-particle tracking produces the transition from the period-two state to the period-one one and vice versa. Here, we see that periodic

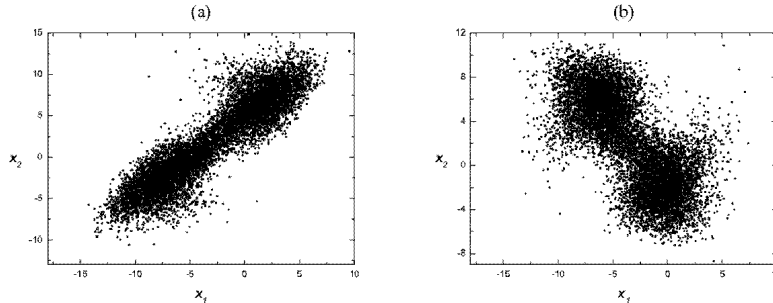


FIG. 6: Phase-space distribution for the period-two state from the multi-particle tracking for the composite wake function. The parameters are given as $\nu = 0.20$, $T_e = 22$, $a = 8$ and $b = 0.18$. (a) and (b) shows the phase space distributions at 19,999 and 20,000 turns, respectively. The equilibrium state shows the same distribution per two turns.

states shown by the Gaussian model also appear in the multi-particle tracking.

As a result, we find that the results from the Gaussian model are in a qualitative agreement with those from the multi-particle tracking in the presence of the linear wake: The existence of the period-doubling bifurcation and the transition between the periodic states. Note that in the present work we only have evaluated the results of the multi-particle tracking for $\nu = 0.2$ in order to show that the simple Gaussian model with the composite wake explains well the behaviors of periodic states and the transition between them, compared to the results from the multi-particle tracking for $0.01 \leq \nu \leq 0.3$.

V. DISCUSSION AND CONCLUSION

In the present work, we have investigated the nonlinear dynamical behaviors and stable periodic states on the longitudinal beam distribution, using both the Gaussian model and multi-particle tracking. It was shown that these periodic states have bifurcations to other periodic states. These behaviors are observed in both the Gaussian model and multi-particle tracking. The model calculations showed the period-one state in the dynamic state of a particle distribution in a beam for the linear wake. It is also confirmed by the multi-particle tracking method. When both the constant wake and linear wake simultaneously exist, the parameter space in which the periodic states exist can be changed by the magnitude of the linear wake. It was concluded that the Gaussian model seems to be useful in investigating qualitatively the particle distribution in the longitudinal phase space.

One of the main purposes in the present work was to investigate the effects of the composite cases taking into account the constant and linear wakes. We examined the dynamical

behaviors of the equilibrium bunch length and their stability for a localized constant and linear wakes. Though the Gaussian model seems to be too simple, the results from the model are in a good agreement with those from the multi-particle tracking method. When both a constant and linear wakes exist in a ring, it was shown that the transition between the periodic states depends on the relative strengths of the two wakes.

Acknowledgments

The work of HChK was supported by Pusan National University. The work of JKA was supported by Korea Institute of Science & Technology Evaluation and Planning(KISTEP) and Ministry of Science & Technology (MOST), Korean government through its BAERI program. JKA is grateful to the PAL, where a part of the present work has been achieved.

-
- [1] K. Hirata: Part. Accel. 22 (1987) 57.
 - [2] K. Hirata, S. Petracca and F. Ruggiero: Phys. Rev. Lett. 66 (1991) 1693.
 - [3] E.-S. Kim and M. Yoon: IEEE Trans. Nucl. Sci. 48 (2001) 181.
 - [4] E.-S. Kim and K. Hirata: KEK Report 95-5 (1995).

TABLE I: Synchrotron tune and stable periodic states for the case of the constant wake function.

Synchrotron tune	Existing periodic state
$0.244 \leq \nu \leq 0.30$	1
$0.153 \leq \nu \leq 0.243$	1; 2; 1-2
$0.103 \leq \nu \leq 0.152$	1; 2; 1-2; 1-3; 2-3
$0.01 \leq \nu \leq 0.102$	1; 2; 1-3; 1-4; 2-3; 1-3-4; 2-3-4